catalysts

MDPI

Article

Stacked Wire Mesh Monoliths for the Simultaneous Abatement of VOCs and Diesel Soot

María Laura Godoy [1], Ezequiel David Banús [1], Oihane Sanz [2], Mario Montes [2], Eduardo Miró [1] and Viviana Guadalupe Milt [1,*]

[1] Instituto de Investigaciones en Catálisis y Petroquímica—INCAPE (UNL, CONICET), Facultad de Ingeniería Química, Santiago del Estero 2829, S3000AOM Santa Fe, Argentina; mgodoy@fiq.unl.edu.ar (M.L.G.); edbanus@fiq.unl.edu.ar (E.D.B.); emiro@fiq.unl.edu.ar (E.M.)

[2] Departamento de Química Aplicada, UFI 56/11, Facultad de Química, Universidad del País Vasco, UPV/EHU, P° Lardizabal, 3, 20018 Donostia, Spain; oihane.sanz@ehu.es (O.S.); mario.montes@ehu.es (M.M.)

* Correspondence: vmilt@fiq.unl.edu.ar; Tel.: +54-342-453-6861

Received: 12 December 2017; Accepted: 8 January 2018; Published: 10 January 2018

Abstract: Structured catalysts based on Pt,CeO_2 deposited on stainless steel wire meshes were developed to build catalytic cartridges for the treatment of diesel exhaust gases. The cartridges were tested for the simultaneous combustion of volatile organic compounds (VOCs) and soot. To this end, *n*-hexane, acetyl acetate, and toluene were selected as probe molecules. Each of them were loaded together with real soot into the cartridges showing that while VOCs abatement takes place between 200 °C and 350 °C, soot combustion occurs in the 300–500 °C temperature range with an average maximum combustion rate at 420 °C. The catalytic cartridges were characterized by scanning electron microscopy (SEM), energy dispersive X-ray spectroscopy (EDS), and Brunauer-Emmett-Teller (BET) techniques. The mechanical stability of the coatings was confirmed by the ultrasound method. Air permeability of the cartridges prepared with different mesh sizes was also measured and the results were correlated using the Payri equation.

Keywords: diesel soot combustion; VOCs abatement; Pt,CeO_2; wire mesh monoliths

1. Introduction

In recent years, a variety of structured catalysts and reactors have been developed both for industrial and environmental applications [1]. Among them, those made of metallic materials deserve special attention due to their advantages when used in very exothermic reactions [2–11]. In particular, wire mesh structures represent a versatile system that can adopt different geometries [12] making them applicable to several industrial and environmental processes. A great variety of wire meshes exist, the more important properties being the mesh opening, the wire diameter, and the material used [2,13,14]. These types of structures have been used in different reactions for volatile organic compound (VOC) combustion [2,15], photocatalysis [16,17], selective catalytic reduction (SCR) of NO_x [18], and also in physical processes, such as oil-water separation [19].

The most popular application of structured catalysts is the abatement of gaseous pollutants coming both from transport vehicles [20–25] and stationary sources. The traditional three-way catalysts used for Otto cycle engines nowadays allow meeting the emission standards for hydrocarbons, nitric oxides, and carbon monoxide. However, in the case of diesel engines, more sophisticated systems are necessary due to the difficulties to eliminate the toxic diesel soot particles and the nitric oxides under lean conditions. Current systems involve an oxidation catalyst, a NO_x trap, a diesel soot filter, and an SCR catalyst that works with urea injection.

Probably the greatest difficulty is to reach the necessary efficiency to eliminate the soot particles in order to accomplish the new EURO standards. Soot particles are composed of a complex mixture of black carbon, metal ashes, hydrocarbons, water, and sulfur compounds. Due to their small size, they can penetrate deep into the human lung producing a cancer risk [26,27]. On the other hand, exhaust gases of diesel engines also contain a variety of harmful VOCs, from C5 to C11, or more [28].

Several catalysts have been studied for soot combustion. Among them, Ce-based ones are probably the most efficient [29]. On the other hand, different types of metallic substrates have been studied in order to develop catalytic systems to abate VOCs and, as mentioned above, wire meshes represent a promising material. Metal mesh substrates combine the excellent mass and heat transfer characteristics with lower manufacturing costs [2]. In a previous work, Banús et al. [13] prepared a new type of wire mesh monoliths that consisted of stacking corrugated wire mesh discs into a metallic cartridge.

The main objective of this study is to develop structured catalysts based on stainless steel stacked meshes in the form of a monolithic cartridge capable of simultaneously burning soot and VOC compounds. The meshes were coated with a Pt,CeO_2 catalyst that was chosen in order to simultaneously eliminate VOCs and soot particles since Pt oxidizes NO to NO_2, which is a stronger oxidant than O_2, and the redox properties of CeO_2 help burning soot with the generated NO_2. The combination of CeO_2 and Pt increases the rate of soot and VOC burning through the creation and stabilization of oxygen species. In this vein, this active phase has been successfully used by Guo et al. [15] for the coating of stainless steel wire meshes as VOC oxidation catalysts. Pt,CeO_2 powder catalyst has also been reported as effective for soot oxidation with NO and O_2 [30]. Toluene, *n*-hexane, and ethyl acetate were chosen as probe molecules, and real diesel soot particles were synthesized and used with the aim of evaluating the efficiency of the proposed system by means of temperature-programmed oxidation experiments. Additionally, the structured catalysts were both chemically and morphologically characterized.

2. Results and Discussion

2.1. Construction of the Catalyst Structures

Stacked metal monoliths were prepared from AISI 304 stainless steel meshes of different mesh size and wire diameter (M1, M2, and M3), whose main characteristics are listed in Table 1. Figure 1a shows photos of the cut meshes with the stamped channel and the empty cylinder used to build the stacked wire mesh monoliths (Figure 1b). Details of the construction steps for this type of metallic monoliths are given elsewhere [1,2,13]. The disposal of the wire meshes allowed obtaining a tortuous structure capable of filtering soot and favoring reactant mixing.

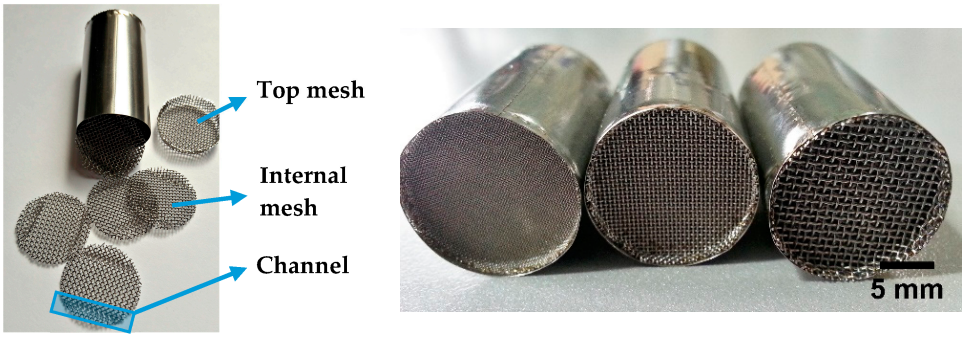

Figure 1. Stacked wire mesh monolith photographs: (**a**) Wire mesh discs with two small transverse channels and cover of the monolith; and (**b**) monolithic cartridges made of different mesh types.

Table 1. Geometric characteristics of the stainless steel AISI 304 wire meshes used to prepare the monoliths.

Wire Mesh Type	M1	M2	M3
Wire diameter (μm)	90	180	250
Mesh-opening (μm)	120	260	500
Geometric surface area (cm^2/g)	54	29	21
Front void fraction (%)	33	35	44

2.2. Catalytic Monoliths: Coating Deposition

The calcination of the stainless steel wire mesh structures at 900 °C for 1 h produced an average increase in weight of 0.20% due to the generation of an oxidic layer, which was composed of spinel structures of Mn, Fe, and Cr, as observed in a previous study [13]. This rough oxidic layer resulted in being well adhered on the surface of the wire meshes, enhancing the thermal stability of the substrate and allowing catalyst anchoring, which shows the importance of this pretreatment prior to the catalyst deposition [31–33].

After the monolith thermal treatment, the washcoating method was applied on structures with 20 and 30 stacked wire meshes, that is, 20 and 30 mm high monoliths, with the aim of incorporating the catalytic coating. This impregnation process using a catalytic nanoparticle suspension (slurry) probed to be adequate to coat wire mesh structures for different applications [34,35]. Figure 2 shows scanning electron microscopy (SEM) images of the different types of CeO_2 nanoparticles composed of the slurry, where grains of sizes <500 nm can be observed both in the commercial CeO_2 nanoparticle sample (CeO_2 Sigma Aldrich®, St. Louis, MO, USA) nanoparticles, denoted as CeO_2-NP) and in the nanoparticle suspension obtained after drying the commercial CeO_2 Nyacol® (Ashland, OR, USA) colloidal suspension (CeO_2-CS). Grains constituting agglomerates >1 μm are observed in the case of the dried and calcined slurry (Figure 2c).

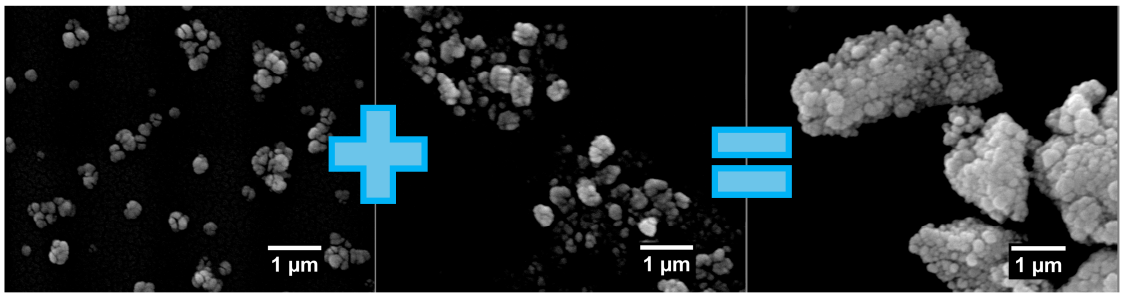

(**a**) (**b**) (**c**)

Figure 2. Scanning electron microscopy (SEM) micrographs of the CeO_2 nanoparticles used for washcoated metallic monoliths: (**a**) commercial CeO_2 Sigma Aldrich® nanoparticles (CeO_2-NP); (**b**) dried commercial CeO_2 Nyacol® suspension (CeO_2-CS); and (**c**) dried and calcined slurry used for washcoated monoliths.

In Figure 3a, the catalyst mass loaded over the substrates versus the number of coating cycles is plotted. The CeO_2 mass loaded increased almost linearly with the successive coatings. Four to five cycles (immersion, centrifugation, drying) were necessary to load 150 mg of CeO_2 using the suspension containing both CeO_2-NP and CeO_2-CS (CeO_2-XMi catalytic monoliths, X indicating the number of stacked wire meshes and Mi the type of wire). On the other hand, only two impregnation steps were needed to achieve 150 mg of CeO_2 loading when using only CeO_2-NP in the suspension (CeO_2*-XMi catalytic monoliths), which is probably related to the higher size of CeO_2 nanoparticles in the slurry compared to the size of nanoparticles that compose the colloidal suspension (CeO_2-CS). In addition,

the number of stacked metal mesh discs also influenced the CeO_2 mass loaded; as expected, the higher the number of stacked wire meshes, the higher the amount of catalyst loaded.

As Figure 3b shows, the washcoating method produced a homogeneous catalytic film over monoliths made from the M3 mesh type, which had the largest wire diameter and highest mesh opening among those studied. Nevertheless, the channels of the monoliths prepared from those meshes with thinner wires and lesser mesh opening, i.e., monoliths constructed from M1 and M2 mesh types, were partially blocked. In view of these results, only monoliths made from M3 wire mesh discs were used for catalytic studies.

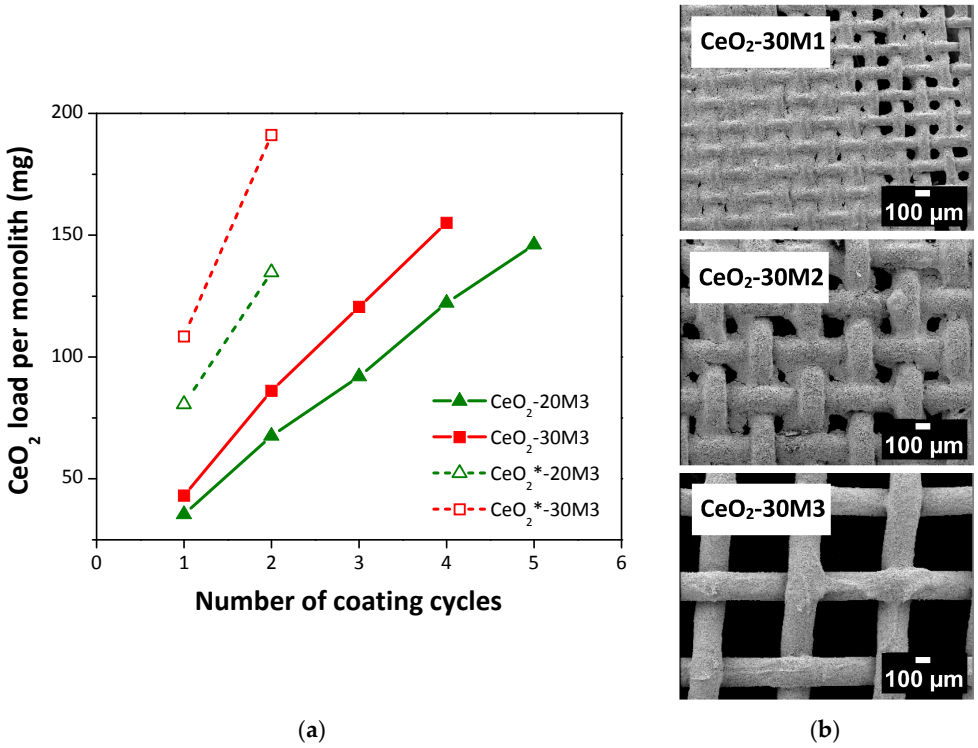

Figure 3. CeO_2 incorporation into metallic monoliths. (**a**) Catalyst mass load vs. coating cycles for structures with different number of stacked M3 type wire meshes, where (*) indicates samples coated with a slurry only containing CeO_2-NP; and (**b**) SEM images of different types of coated wire meshes after CeO_2 loading.

2.3. Characterization of Catalytic Structures

SEM images of top and inner meshes of the monolith made from 30 stacked M3 type wire meshes after the different stages of preparation are shown in Figure 4. The deposition of the CeO_2 coating resulted in a homogeneous film, composed of conglomerates of particles of variable size, ranging from 1 to 10 µm, which completely covered the metallic wires.

For the catalyst containing both CeO_2 and Pt (Pt,CeO_2-30M3), both meshes set at the top and in the middle of the monolith were analyzed in order to study the homogeneity of the impregnation procedure. It can be observed that the Pt,CeO_2 coating seems to be homogeneous and well adhered, so in the top, as in the middle meshes of the 30M3 monolith (Figures 4 and 5), Pt appeared well distributed all along the metallic wires.

Table 2 shows semi-quantitative percentages of components detected by energy dispersive X-ray spectroscopy (EDS), both from line scanning and mapping analysis of zones denoted in Figure 5. Although a visual inspection of the EDS mapping pictures shown in Figure 5 suggests a homogeneous distribution of the elements on the wire meshes, there are some differences from the line scanning and the mapping values (in between parenthesis), which indicates some heterogeneity in the distribution

of components in the coating. More significant differences appear when comparing the top and the middle meshes of the cartridge, which could be ascribed to the thicker coating obtained in the middle of the monolith, as a result of the centrifugation process. As previously stated, the thermal treatment of the meshes increased the concentration of Cr and Mn on the mesh surface, from 17.0 to 34.2 the wt % of Cr, and from less than 0.5 to 6.8 wt % the Mn content. After the coating with CeO_2, as expected, the surface concentration of Fe, Cr, and Mn decreased, and after Pt incorporation, these relative concentrations varied, probably associated with the analysis depth of the technique (1–3 µm). It is important to remark that the EDS technique allowed the detection of Pt (Table 2 and Figure 5) and that the Pt,CeO_2 concentration, from mapping results, is close to 1 wt %.

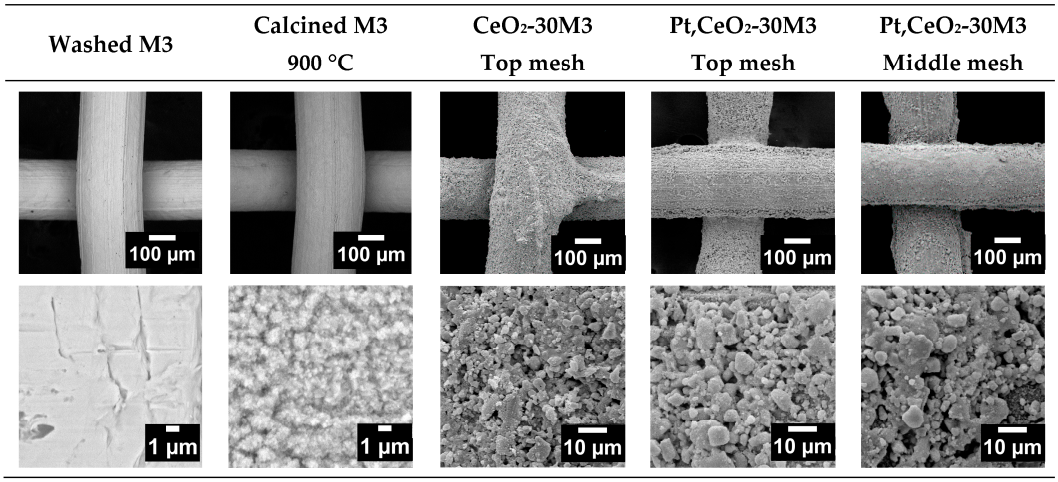

Figure 4. SEM images of Pt,CeO_2-30M3 meshes after the different steps of preparation of the catalytic monolith.

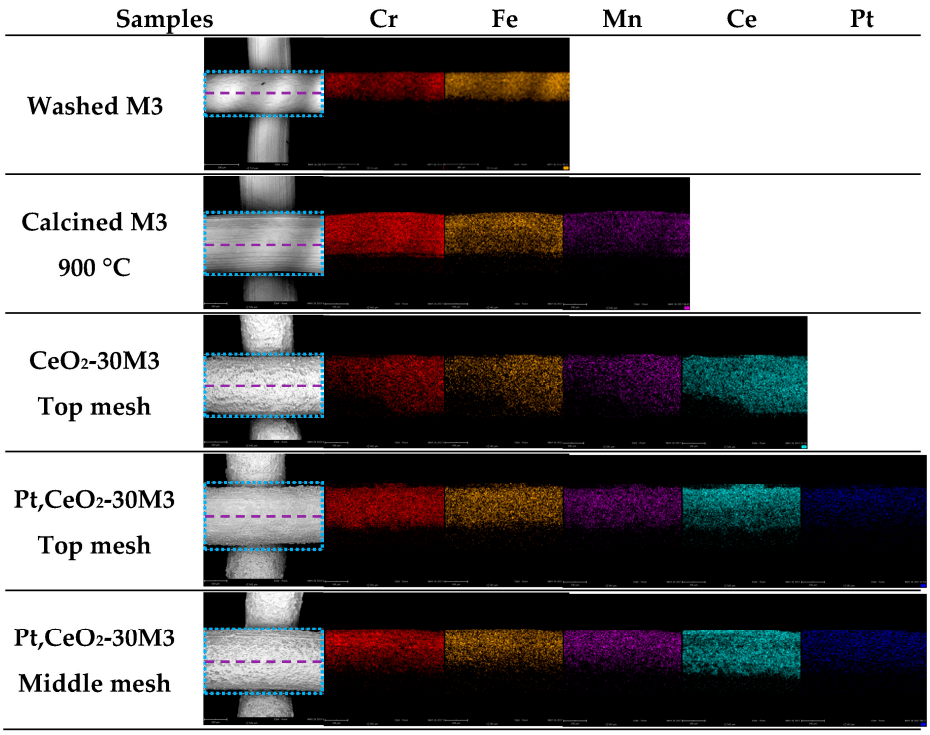

Figure 5. EDS mapping images of M3 meshes after the different steps of preparation of the catalytic monolith Pt,CeO_2-30M3.

Table 2. Elemental composition from energy dispersive X-ray spectroscopy (EDS) analysis of line scanning indicated in Figure 5 (weight %) [a].

	AISI 304 Composition [b]	Washed M3	Calcined M3	CeO_2-30M3 Top Mesh	Pt,CeO_2-30M3 Top Mesh	Pt,CeO_2-30M3 Middle Mesh
Cr	18–20	17.0 (16.4)	34.2 (27.8)	2.9 (3.5)	18.2 (13.8)	7.6 (9.5)
Fe	66–74	67.1 (65.4)	22.3 (21.9)	1.5 (2.0)	13.1 (9.1)	4.1 (7.2)
Mn	<2	n.d. [c]	6.8 (5.3)	<0.5	3.5 (2.7)	0.5 (1.0)
Ce	-	-	-	76.7 (74.2)	31.6 (45.1)	70.9 (55.2)
Pt	-	-	-	-	2.4 (<0.5)	<0.5 (<0.5)

[a] Values between parenthesis were obtained from mapping areas indicated in Figure 5; [b] Nominal composition; [c] Non-detectable.

Related to textural properties, Table 3 shows the Brunauer–Emmett–Teller (BET) surface area values both of powder and structured catalysts. For the slurry dried and calcined at 600 °C (Pt,CeO_2-P), the surface area was 64.4 m^2/g, whereas when using only nanoparticles (CeO_2-NP), the BET surface area of the calcined slurry (Pt,CeO_2*-P) decreased to 33 m^2/g. This difference is related to the presence of the higher surface area colloidal CeO_2 used as an additive for the slurry preparation [36]. Both the structured catalyst made from 20 or 30 stacked wire meshes present similar BET surface area values, around 24 m^2/g, that correspond to the catalytic layer since that of the uncoated calcined monolith is negligible.

Table 3. Textural properties of the different samples.

Sample [a]		BET Surface (m^2/g)
Powder catalyst	Pt,CeO_2-P	64.4
	Pt,CeO_2*-P	33.3
Structured catalyst	Pt,CeO_2-20M3	23.8
	Pt,CeO_2-30M3	23.6

[a] Powder catalysts consist on the dried and calcined (at 600 °C) slurries with (Pt,CeO_2-P) and without (Pt,CeO_2*-P) the addition of CeO_2 nanoparticle commercial colloidal suspension. Structured catalysts consist on metallic monoliths of different lengths (20 and 30 mm) loaded with the Pt,CeO_2 catalyst.

On the other hand, Figure 6 presents the pressure drop of the wire mesh monoliths. The permeability curves of monoliths with different number of wire mesh discs with M1, M2, and M3 mesh types are shown in Figure 6a. It can be seen that the flow (Q) increases when the number of stacked metal discs decreases, at the same pressure drop (ΔP) value. Additionally, Q increases as the mesh opening does when the height of the structures is maintained. Figure 6b shows straight lines obtained when plotting $\Delta P/Q$ vs. Q, according to the model proposed by Payri et al. (see Equation (1)) for diesel particulate filters (DPF) [37]. Parameters of this model take into account differences in pressure due to changes in the section of the flow channels (b) and also those caused by the flow through the porous catalytic layer (a). Note the high values of Q obtained, which denote the high permeability of the wire mesh structures, although, as expected, the addition of the catalyst diminishes the flow area thus increasing ΔP.

$$\text{Payri equation}: \Delta P_{DPF} = aQ + bQ^2 \quad (1)$$

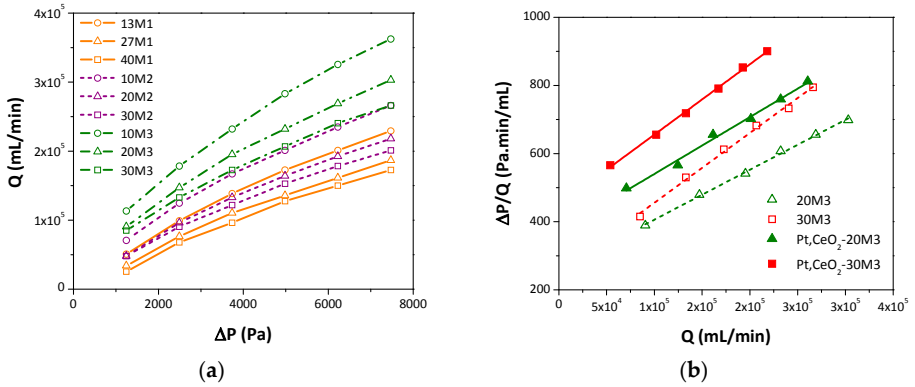

Figure 6. Pressure drop of the wire mesh monoliths: (**a**) calcined at 900 °C with 10, 20, and 30 stacked M1, M2, and M3 mesh discs; (**b**) before and after the Pt,CeO_2 coating.

2.4. Catalyst Performance of the Stacked Wire Mesh Monoliths: Soot Combustion and VOC Removal

Temperature-programmed oxidation (TPO) experiments were performed with 20 and 30 stacked wire mesh structures (Pt,CeO_2-XM3) and the catalytic activity was evaluated for the two oxidation reactions of environmental interest considered: VOCs and diesel soot abatement. In a first series of experiments, different volatile organic compounds were used as solvents to prepare soot suspensions, which were used to simultaneously incorporate soot and VOCs into the monolithic structure.

Firstly, *n*-hexane was used for this purpose. In order to study the effects of the commercial colloidal CeO_2 nanoparticles suspension (CeO_2-CS) on soot combustion activity, catalytic tests of structured substrates coated either with the slurry containing both CeO_2-NP and CeO_2-CS nanoparticles (Pt,CeO_2-XM3) or when using only CeO_2-NP in the coating suspension (Pt,CeO_2*-XM3) were carried out (Figure 7). It can be noticed that all the samples present similar temperature of maximum soot combustion rates of nearly 420 °C, whereas the temperature of maximum burning of *n*-hexane occurs at ca. 250 °C. However, the adherence tests carried out on those samples (Figure 8) indicated the poor retention of the CeO_2-NP coating (around 60% for Pt,CeO_2*-30M3) after 210 min of sonication, whereas the inclusion of the colloidal suspension produced well-adhered coatings (retention > 90%). Taking into account the smaller particle size of CeO_2-CS, it allows the adhesion of CeO_2-NP nanoparticles, thus producing a stable coating. Therefore, the suspension composed of both CeO_2-NP and CeO_2-CS nanoparticles was chosen for further catalytic studies.

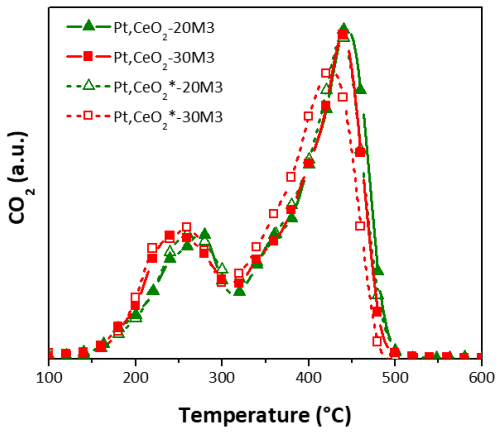

Figure 7. Catalytic tests carried out with 20 and 30 mesh structures, loaded using the slurry containing CeO_2-NP and CeO_2-CS (solid symbols) and using the slurry containing only CeO_2-NP (open symbols, * samples). Soot and *n*-hexane were loaded to the wire mesh monoliths from a suspension of soot in *n*-hexane.

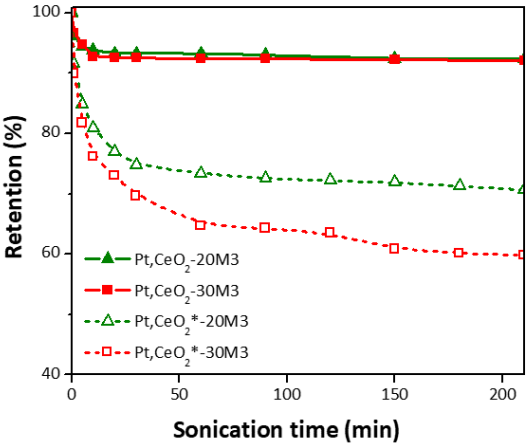

Figure 8. Adherence tests carried out on Pt,CeO_2-monoliths made from different numbers of stacked wire meshes, coated with the slurry containing both CeO_2-CS and CeO_2-NP (solid symbols) or only CeO_2-NP (open symbols, * samples).

In order to check the catalytic activity of the bare catalytic formulation, i.e., the catalytic powder not deposited on the structured substrate, the slurry was dried and calcined after which Pt was incorporated (Pt,CeO_2-P). In this case, the maxima for soot combustion are observed at 420 °C and 470 °C for tight and loose soot to catalyst contact respectively (see Figure 9), though the last peak presents a shoulder at 420 °C, indicating that soot is partially burnt under tight conditions also when loosely mixing the powder catalyst and soot. It is worth noting that the activity of the powder catalyst in tight contact with soot was preserved after its incorporation into the monolith.

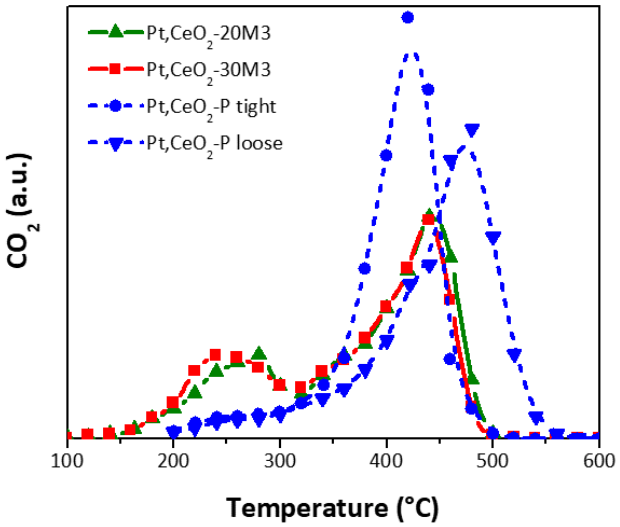

Figure 9. Catalytic activity of monoliths with 20 and 30 stacked M3 wire meshes compared to that of the powder catalyst (tight and loose contact) for soot combustion.

Secondly, ethyl acetate as VOC was used to incorporate soot into the structured catalysts, using for this purpose a soot suspension containing 3000 ppm. Figure 10 shows the simultaneous soot and VOC combustion curves. It can be clearly observed that, in this case, the two maxima appear at 270 °C and 420 °C, the first peak corresponding to the ethyl acetate ignition and the second one to the soot combustion.

Finally, the use of the suspension of soot in toluene allows checking of the simultaneous soot and toluene combustion. In this case, the maximum VOC combustion temperature was observed at around

300 °C, both for monoliths made from 20 or 30 stacked wire meshes (Figure 11), whereas soot burns with a maximum rate at 420 °C.

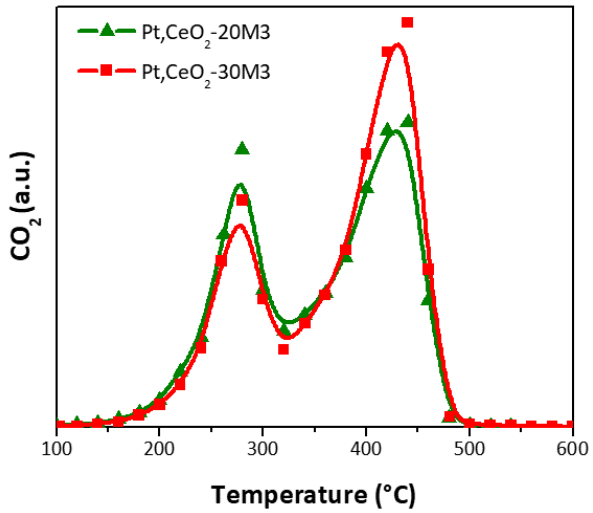

Figure 10. Simultaneous soot and ethyl acetate combustion using catalytic stacked wire mesh monoliths.

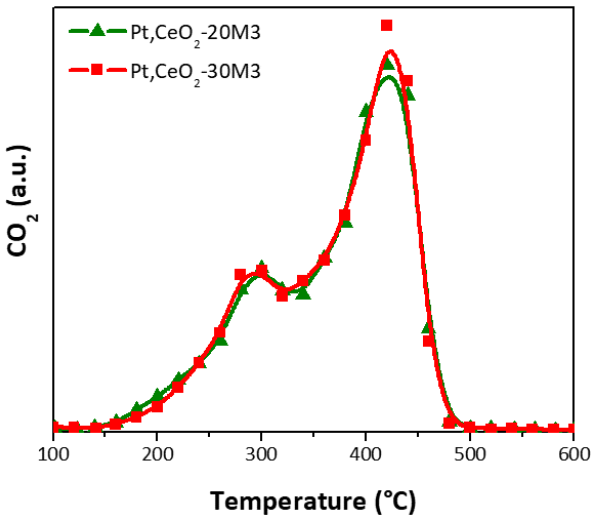

Figure 11. Simultaneous toluene and soot combustion on catalytic stacked wire mesh monoliths.

As Figure 12 shows, all the studied VOC compounds are completely oxidized at temperatures below 350–370 °C, being the maximum combustion temperatures for *n*-hexane < ethyl acetate < toluene, when using the Pt,CeO_2-30M3 catalyst. Nevertheless, the presence of these different VOC only slightly affects the soot combustion maximum temperature. Some displacement of TPO curves in the soot combustion zone could be ascribed to different soot-catalyst contact types obtained with the different VOC solvents.

Additionally, Figure 13 displays the conversion profiles for ethyl acetate ignition under continuous feed conditions, using both the powder and the structured catalysts. Both Pt,CeO_2-20M3 and Pt,CeO_2-30M3 exhibit similar profiles, where the light off curves start at ca. 200 °C, reaching 100% ethyl acetate conversion at 280 °C. Although the beginning of the ethyl acetate combustion starts at lower temperatures for the powder catalyst, the 100% conversion occurs at temperatures higher than 300 °C, associated to the higher dispersion of the catalyst in the structured system.

The presence of Ce active species in the mesh surface (Pt,CeO_2-30M3 top and middle meshes—Figure 5) after the Pt addition can explain the high activity of the Pt,CeO_2 structured catalysts. It has been demonstrated that cerium oxide is an oxygen supplier in oxidation reactions, and the oxygen vacancies formed favor the catalytic activity. Ceria plays a synergistic effect by stabilizing Pt species and creating vacancies over the wire mesh support [15,38,39]. Additionally, the presence of Fe, Cr, and Mn species lower the soot oxidation temperatures [29].

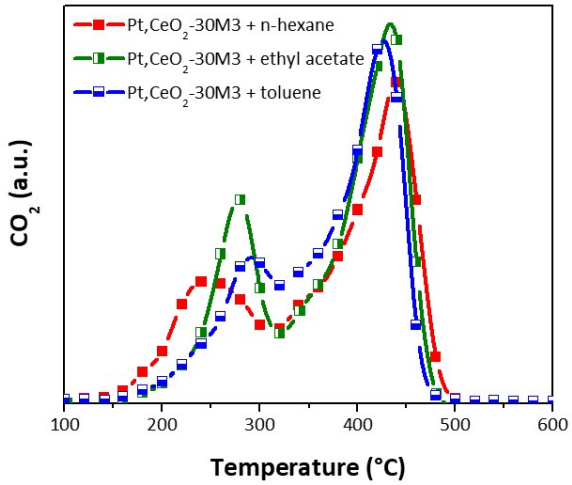

Figure 12. Temperature-programmed oxidation (TPO) curves for the simultaneous soot and VOCs combustion.

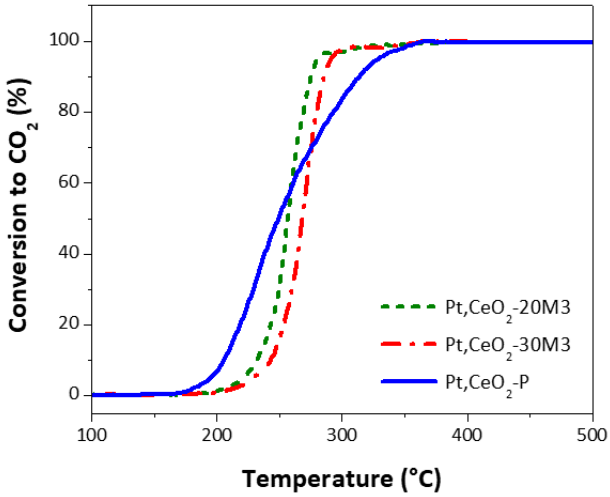

Figure 13. TPO curves for the ethyl acetate combustion under continuous feed conditions, using powdered and structured catalysts.

In order to compare with some results reported in the literature, e.g., Sanz et al. [2], the parallel channels and stacked wire mesh monoliths were studied for toluene and methanol elimination. A washcoating procedure was used for coating Pt, cryptomelane (manganese octahedral molecular sieve, OMS-2) catalyst over two types of metallic monoliths. It was demonstrated that the stacked wire mesh monoliths presented higher activity than parallel channel monoliths, because of the better mixing of reactants due to the tortuosity of the narrow porous substrate structure. The temperature for 50% of conversion in the catalytic oxidation of toluene was 240 °C for the stacked mesh monoliths. Guo et al. [15] prepared similar structured catalysts of 0.1% Pt—0.75% CeO_2/stainless steel wire meshes. The surface of the substrate was modified via anodic oxidation, thus providing a favorable

condition for the posterior anchoring of platinum and ceria active species. The complete oxidation temperatures for toluene and ethyl acetate were 240 °C and 300 °C, respectively, values close to those achieved in our test results. Other similar results were reported by Gómez et al. [36], who prepared a Co/La-CeO_2 formulation, powdered and washcoated onto cordierite honeycomb catalysts. In this case, the temperatures for 50% of conversion in the catalytic oxidation of toluene and ethyl acetate over the structured samples were approximately 250 °C and 245 °C. Additionally, aluminum wire meshes coated with Co-Mn-Al and Co oxides were prepared by Jirátová et al. [40], which showed a high catalytic activity for deep ethanol oxidation.

On the other hand, wire mesh substrates were used in catalytic converters to reduce exhaust emissions, e.g., a copper-based catalytic converter was assembled by Amin et al., using wire meshes coated with copper by electroplating [41]. The light-off temperature obtained was 230 °C to 250 °C, lower values than those we obtained using a noble metal. By using a copper-based catalytic converter it was found that HC was reduced by 38% and CO by 33% at full load. Another catalytic converter was developed consisting of a TiO_2/CoO coating over stainless steel wire mesh substrates [42]. The meshes were first coated with the metal catalysts by a washcoating technique and then arranged into a straight bar. It was found that the conversion efficiencies were 93%, 89%, and 82% for NO_x, CO, and HC emissions, respectively, and the light-off temperature was 270 °C to 360 °C, thus, the resulting TiO_2/CoO oxide-based catalytic converter is very effective for natural gas direct injection engines. Kumar et al. [43] developed a new catalytic converter using ZrO/CoO washcoated over wire mesh substrates. The experiments on a petrol engine showed that the percentage reduction of pollution content CO, HC, and NO_x was 53%, 65%, and 39%, respectively.

3. Materials and Methods

3.1. Construction of the Stacked Wire Mesh Monoliths

The stacked wire mesh monoliths were assembled according to the procedure described by Banús et al. [13]. Different types of AISI 304 wire meshes (provided by Rey and Ronzoni) were used, whose geometric characteristics are shown in Table 1. AISI 304 stainless steel cylindrical cartridges were made by spot-welding (50 µm thickness, Goodfellow®, Coraopolis, PA, USA), 16 mm in diameter and variable height, according to the number of stacked wire mesh discs of the monolith (20–30 discs that were traduced in structures of 20–30 mm in height).

Two different homemade stainless steel matrices were used to cut and corrugate the internal wire mesh discs by stamping, producing two small parallel channels (Figure 1a). These channels let the internal discs maintain separation (0.15–0.30 mm) when they were 90° alternatively stacked, thus making it easier the ulterior coating process with the catalyst suspension and promoting the flow of gases inside the monolith. Top meshes were cut and folded and then spot-welded to the cartridge to close the structure. Figure 1b shows the stacked wire mesh monoliths made using the three different types of wire meshes explored.

The metallic monoliths were initially washed in detergent-water in an ultrasonic bath for 30 min, and then in acetone under the same conditions. The substrates were dried in an oven at 130 °C for 2 h after each washing step.

3.2. Pretreatment of the Structured Substrates

After the construction stage, a pretreatment was necessary to generate a rough surface that promotes the catalyst adherence to the substrate [44]. This was performed by calcining the stacked wire mesh monoliths at 900 °C for 1 h in a furnace (heating rate 10 °C/min) [32]. The resulting rough oxidic layer also protected the metallic structure. Calcinated monoliths were designated as XMi, where X is the number of stacked wire meshes and Mi the type of mesh used (e.g., 30M3).

3.3. Catalyst Preparation and Washcoating of the Structures

The washcoating method was carried out by dipping the wire mesh structured substrates into a CeO_2 suspension, composed of a mixture of CeO_2 nanoparticles, CeO_2-NP (Sigma Aldrich®, St. Louis, MO, USA), $d_{particle}$ < 50 nm) and CeO_2 commercial colloidal suspension, CeO_2-CS (Nyacol®, 20 *w/wt* %, $d_{particle}$ = 10–20 nm, pH = 3). Briefly, 0.5 g of polyvinyl alcohol (PVA, Sigma Aldrich®) was dissolved in 25 mL of deionized water, previously heated at 70 °C under magnetic stirring. Afterwards, 25 g of CeO_2-CS, and then 5 g CeO_2-NP were slowly added to the aqueous solution at room temperature. The suspension remained under stirring for 24 h, pH = 3. PVA was used to decrease the surface tension of the slurry, thus enhancing the contact between the slurry and the wire meshes.

Before the coating process, the external surface of the monoliths was first masked with Teflon® (Buenos Aires, Argentina) tape and then with heat-shrinkable tape to produce the catalyst layer preferably on the wire meshes and the internal area of the cylinder. Posterior to 1 min immersion of the covered cartridges into the ceria suspension, the elimination of the excess slurry was carried out by centrifugation at 600 rpm for 3 min (relative centrifugal force, RCF = 36.5 g), with a HERMLE Z 326 centrifuge. After that, the structures were dried for 1 h at 120 °C in an oven and then weighed. The complete process (impregnation plus drying) was carried out several times using the same slurry until the CeO_2 loading was around 150 mg. Next, the coated monoliths were calcined in a furnace (heating rate 1 °C/min) for 2 h at 600 °C. These samples were named as CeO_2-XMi (e.g., CeO_2-30M3).

Finally, 1 wt % Pt (referred to the CeO_2 mass loaded) was added to the CeO_2 coated monoliths by the wetness impregnation method. An aqueous solution was prepared dissolving 0.1 g of $Pt(NH_3)_4(NO_3)_2$ (Sigma Aldrich®) in 25 mL of deionized water, under magnetic stirring. As in the previous stage, the external surface of the structures was covered with Teflon® and heat-shrinkable tape. The samples were immersed in a volume of the Pt solution so as to exactly fill the volume of the pores. After that, the samples were dried at 120 °C and calcined 2 h at 600 °C. This procedure was repeated until reaching 1 wt % of Pt, referred to as the washcoating mass. In this way, catalytic monoliths were obtained, designated as Pt,CeO_2-XMi (e.g., Pt,CeO_2-30M3).

In addition to the structured catalysts, a powder formulation—1 wt % Pt,CeO_2—was obtained. To this aim, the same CeO_2 suspension (slurry used for the immersion of the monoliths) was first dried at 120 °C and then calcined at 600 °C for 2 h, after which 1 wt % Pt was added from the $Pt(NH_3)_4(NO_3)_2$ aqueous solution. The Pt,CeO_2 suspension was heated at 70 °C under magnetic stirring until dryness and, lastly, it was calcined at 600 °C for 2 h. The catalyst was called Pt,CeO_2-P.

On the other hand, another suspension was prepared containing only CeO_2-NP—that is, without the addition of CeO_2-CS—but containing the same amount of cerium. To this aim, 10 g of CeO_2 Aldrich nanoparticles were dispersed into the PVA aqueous solution with continuous stirring. The suspension obtained was stirred for 24 h before the coating of the monoliths. The complete process (impregnation plus drying) was repeated until the CeO_2 mass load was around 150 mg and subsequently 1 wt % of Pt was incorporated, as previously described. A calcination stage at 600 °C for 2 h before and after this step was necessary. The catalytic structures thus obtained were denominated Pt,CeO_2*-XMi (e.g., Pt,CeO_2*-30M3).

3.4. Characterization of the Catalysts

The morphology of powders and catalytic structures was determined by scanning electron microscopy (SEM) using a JEOL JSM-35C microscope. Previously, the samples were gold-covered by sputtering, using a SPI SUPPLIES model SPI 12157-AX system.

The adherence of the Pt,CeO_2 coating deposited onto the stacked wire mesh monoliths was tested by ultrasound. To this aim, coated samples were immersed in acetone and sonicated for different times at room temperature [45]. After that, the samples were dried at 120 °C for 1 h and weighed. This treatment was repeated until no additional weight loss was observed. Results are displayed in terms of the retained amount of the Pt,CeO_2 layer on the monolithic structure, expressed as a percentage.

The coating composition was analyzed by energy dispersive X-ray spectroscopy (EDS), using a SEM Phenom World PRO X instrument (Phenom-World, Eindhoven, The Netherlands).

The textural characterization of structured and powdered catalysts was determined by nitrogen physisorption using a Micromeritics ASAP 2020 instrument (Micromeritics Instrument Corporation, Norcross, GA, USA). The samples were degassed at 300 °C for 2 h prior to the analysis. In the case of structured catalysts, the whole monolith was analyzed, using for this purpose a special sample cell. The surface area was determined by the BET (Brunauer–Emmett–Teller) method and results are reported per gram of catalyst.

Permeability tests of the monoliths were performed in a Flujo Tech 600 flowmeter (Horacio Resio Devices, Buenos Aires, Argentina) [46] which is used for flow measurements in real engine exhausts. With the aim of using this equipment for the cartridges studied here, it was necessary to construct a device to adapt them to the sample holder. The software program of the equipment displayed the flow curves (cfm, cubic feet per minute) for different pressure values (inch/H_2O).

3.5. Catalytic Tests

The catalytic activity of the different samples for the oxidation of soot and VOCs (ethyl acetate, *n*-hexane, acetone, and toluene) was studied by means of temperature-programmed oxidation (TPO). Activity profiles were plotted, normalized according to the total area of CO_2.

3.5.1. Simultaneous Soot and VOC Combustion

The burning of commercial diesel fuel (YPF, Argentina) in a glass vessel allowed collecting soot particles from the vessel walls, which were dried in a stove at 120 °C for 72 h [47] and then dispersed in appropriate solvents using an ultrasonic bath. Selected VOCs were used as solvents: *n*-hexane, ethyl acetate, and toluene. Soot and the corresponding VOC were incorporated into the structured catalysts from each of these suspensions.

Firstly, the external surface of the cartridges was covered to avoid the deposition of soot on the external metallic foil. Secondly, the wire mesh monoliths were immersed into the soot suspension (3000 ppm) for 1 min and dried at room temperature for 20 min, thus obtaining samples loaded both with soot and the corresponding VOC. The aim of these experiments was to obtain a soot-to-catalyst contact similar to that obtained under real applications [48] and use the samples to simultaneously study the burning of soot and the corresponding VOC.

The tubular reactor was fed with 20 mL/min of a mixture of NO (0.1%) and O_2 (18%), He balance, with a heating rate of 5 °C/min. A Shimadzu GC-2014 gas chromatograph with a Porapak Q column was used for the analysis of the gaseous products (O_2 and CO_2).

The activity of powder formulations for the combustion of soot was evaluated under both loose and tight contact conditions, mixing the appropriate amounts of soot and the catalyst so as to obtain a soot/catalyst ratio = 1/20 (*w*/*w*). The loose contact was achieved simply by mixing the soot and the catalyst with a spatula, whereas the soot and the powder catalysts were mechanically mixed in an agate mortar for three minutes so as to obtain tight contact conditions.

3.5.2. VOC Oxidation

To further study ethyl acetate combustion under continuous feed conditions, both the powder and the structured catalyst were tested in a tubular fixed-bed reactor at atmospheric pressure. The feeding composition was 500 mL/min of an air stream containing 500 mgC/m^3 of VOC (ethyl acetate) with a heating rate of 2 °C/min. Conversion values were obtained by measuring the CO_2 production through an online detector (Vaisala GMT220, Vaisala Corporation, Helsinki, Finland).

4. Conclusions

The washcoating technique allowed obtaining catalytic coatings rather well distributed over stainless steel wire meshes.

The permeability of the wire mesh monoliths was good enough to avoid a pressure drop if these structures are considering as potential candidates for diesel particulate filters.

It was necessary to use the colloidal CeO_2 in the slurry formulation to obtain good adhesion. Fortunately, our results show that the use of this colloid slightly increases catalytic activity.

Pt,CeO_2 deposited on wire mesh structures showed good activity for the simultaneous combustion of VOCs and soot, burning the solvents in the 200–350 °C temperature range and the soot particles between 300 °C and 500 °C, with an average maximum temperature peak at 420 °C, which makes this system promising for the development of catalytic combustors and diesel soot filters.

Acknowledgments: The authors wish to acknowledge the financial support received from ANPCyT, CONICET and UNL (Argentina), the Basque Government (IT1069-16), and the Spanish MINECO/FEDER (ENE2015-66975-C3-3-R and CTQ2015-73901-JIN).

Author Contributions: María Laura Godoy constructed metallic structures and prepared the catalytic monoliths. She also performed catalytic evaluations for the simultaneous removal of soot and VOC compounds. Ezequiel Banús and Oihane Sanz evaluated the ethyl acetate oxidation under continuous flow and determined some of the textural properties of the catalysts. Viviana Guadalupe Milt and Eduardo Miró designed and supervised experiments in Argentina and Mario Montes directed the tests carried out in Spain. Finally, María Laura Godoy and Viviana Milt wrote the article with the agreement of the other authors.

Conflicts of Interest: The authors declare no conflict of interest.

References

1. Avila, P.; Montes, M.; Miró, E.E. Monolithic reactors for environmental applications: A review on preparation technologies. *Chem. Eng. J.* **2005**, *109*, 11–36. [CrossRef]
2. Sanz, O.; Banús, E.D.; Goya, A.; Larumbe, H.; Delgado, J.J.; Monzón, A.; Montes, M. Stacked wire mesh monoliths for VOCs combustion: Effect of the mesh-opening in the catalytic performance. *Catal. Today* **2017**. [CrossRef]
3. Merino, D.; Sanz, O.; Montes, M. Effect of the thermal conductivity and catalyst layer thickness on the Fischer-Tropsch synthesis selectivity using structured catalysts. *Chem. Eng. J.* **2017**, *327*, 1033–1042. [CrossRef]
4. Sheng, M.; Yang, H.; Cahela, D.R.; Tatarchuk, B.J. Novel catalyst structures with enhanced heat transfer characteristics. *J. Catal.* **2011**, *281*, 254–262. [CrossRef]
5. Sheng, M.; Yang, H.; Cahela, D.R.; Yantz, W.R.; Gonzalez, C.F.; Tatarchuk, B.J. High conductivity catalyst structures for applications in exothermic reactions. *Appl. Catal. A Gen.* **2012**, *445–446*, 143–152. [CrossRef]
6. Tronconi, E.; Groppi, G.; Visconti, C.G. Structured catalysts for non-adiabatic applications. *Curr. Opin. Chem. Eng.* **2014**, *5*, 55–67. [CrossRef]
7. Groppi, G.; Tronconi, E. Design of novel monolith catalyst supports for gas/solid reactions with heat exchange. *Science* **2000**, *55*, 2161–2171. [CrossRef]
8. Groppi, G.; Tronconi, E. Honeycomb supports with high thermal conductivity for gas/solid chemical processes. *Catal. Today* **2005**, *105*, 297–304. [CrossRef]
9. Visconti, C.G.; Groppi, G.; Tronconi, E. Highly conductive "packed foams": A new concept for the intensification of strongly endo- and exo-thermic catalytic processes in compact tubular reactors. *Catal. Today* **2016**, *273*, 178–186. [CrossRef]
10. Visconti, C.G.; Tronconi, E.; Groppi, G.; Lietti, L.; Iovane, M.; Rossini, S.; Zennaro, R. Monolithic catalysts with high thermal conductivity for the Fischer-Tropsch synthesis in tubular reactors. *Chem. Eng. J.* **2011**, *171*, 1294–1307. [CrossRef]
11. Razza, S.; Heidig, T.; Bianchi, E.; Groppi, G.; Schwieger, W.; Tronconi, E.; Freund, H. Heat transfer performance of structured catalytic reactors packed with metal foam supports: Influence of wall coupling. *Catal. Today* **2016**, *273*, 187–195. [CrossRef]
12. Hernández-Giménez, A.; Lozano Castelló, D.; Bueno-López, A. Diesel soot combustion catalysts: Review of active phases. *Chem. Pap.* **2014**, *68*, 1154–1168. [CrossRef]
13. Banús, E.D.; Sanz, O.; Milt, V.G.; Miró, E.E.; Montes, M. Development of a stacked wire mesh structure for diesel soot combustion. *Chem. Eng. J.* **2014**, *246*, 353–365. [CrossRef]

14. Zagoruiko, A.N.; Lopatin, S.A.; Mikenin, P.E.; Pisarev, D.A.; Zazhigalov, S.V.; Baranov, D.V. Novel structured catalytic systems—Cartridges on the base of fibrous catalysts. *Chem. Eng. Process. Process Intensif.* **2017**. [CrossRef]
15. Guo, H.; Xue, B.; Chen, M. Catalytic oxidation of VOCs over the structured bimetallic catalyst 0.1% Pt-0.75% CeO_2/SSWM. *Sustain. Environ. Res.* **2015**, *25*, 167–170.
16. Hsu, M.H.; Chang, C.J. Ag-doped ZnO nanorods coated metal wire meshes as hierarchical photocatalysts with high visible-light driven photoactivity and photostability. *J. Hazard. Mater.* **2014**, *278*, 444–453. [CrossRef] [PubMed]
17. Jing, W.; Cheng, Y.; Gao, W.; Jiang, Z.; Jiang, K.; Shi, J.; Zhou, F. Different photo-catalytic degradation of methylene blue by varied ZnO nanorods on dissimilar stainless steel wire sieves. *Mater. Res. Bull.* **2017**, *86*, 313–321. [CrossRef]
18. Boukha, Z.; De La Torre, U.; Pereda-Ayo, B.; González-Velasco, J.R. Catalytic properties of CuO/Al_2O_3-based microreactors in SCR of NO_x with NH_3. *Top. Catal.* **2016**, *59*, 1002–1007. [CrossRef]
19. Song, B. Simple and fast fabrication of superhydrophobic metal wire mesh for efficiently gravity-driven oil/water separation. *Mar. Pollut. Bull.* **2016**, *113*, 211–215. [CrossRef] [PubMed]
20. Fino, D.; Bensaid, S.; Piumetti, M.; Russo, N. A review on the catalytic combustion of soot in Diesel particulate filters for automotive applications: From powder catalysts to structured reactors. *Appl. Catal. A Gen.* **2016**, *509*, 75–96. [CrossRef]
21. Banús, E.D.; Milt, V.G.; Miró, E.E.; Ulla, M.A. Structured catalyst for the catalytic combustion of soot: Co,Ba,K/ZrO_2 supported on Al_2O_3 foam. *Appl. Catal. A Gen.* **2009**, *362*, 129–138. [CrossRef]
22. Banús, E.D.; Milt, V.G.; Miró, E.E.; Ulla, M.A. Co,Ba,K/ZrO_2 coated onto metallic foam (AISI 314) as a structured catalyst for soot combustion: Coating preparation and characterization. *Appl. Catal. A Gen.* **2010**, *379*, 95–104. [CrossRef]
23. Banús, E.D.; Ulla, M.A.; Miró, E.E.; Milt, V.G. Co,Ba,K/ZrO_2 coated onto metallic foam (AISI 314) as a structured catalyst for soot combustion: Catalytic activity and stability. *Appl. Catal. A Gen.* **2011**, *393*, 9–16. [CrossRef]
24. Tuler, F.E.; Portela, R.; Ávila, P.; Banús, E.D.; Miró, E.E.; Milt, V.G. Structured catalysts based on sepiolite with tailored porosity to remove diesel soot. *Appl. Catal. A Gen.* **2015**, *498*, 41–53. [CrossRef]
25. Tuler, F.E.; Banús, E.D.; Zanuttini, M.A.; Miró, E.E.; Milt, V.G. Ceramic papers as flexible structures for the development of novel diesel soot combustion catalysts. *Chem. Eng. J.* **2014**, *246*, 287–298. [CrossRef]
26. Guan, B.; Zhan, R.; Lin, H.; Huang, Z. Review of the state-of-the-art of exhaust particulate filter technology in internal combustion engines. *J. Environ. Manag.* **2015**, *154*, 225–258. [CrossRef] [PubMed]
27. Boningari, T.; Smirniotis, P.G. Impact of nitrogen oxides on the environment and human health: Mn-based materials for the NO_x abatement. *Curr. Opin. Chem. Eng.* **2016**, *13*, 133–141. [CrossRef]
28. Alves, C.A.; Lopes, D.J.; Calvo, A.I.; Evtyugina, M.; Rocha, S.; Nunes, T. Emissions from light-duty diesel and gasoline in-use vehicles measured on chassis dynamometer test cycles. *Aerosol Air Qual. Res.* **2015**, *15*, 99–116. [CrossRef]
29. Mohankumar, S.; Senthilkumar, P. Particulate matter formation and its control methodologies for diesel engine: A comprehensive review. *Renew. Sustain. Energy Rev.* **2017**, *80*, 1227–1238. [CrossRef]
30. Song, S.; Jung, J.; Song, S.; Chun, K.M. Experimental study of soot oxidation characterization of Pt/CeO_2 catalyst with NO and O_2 using a flow reactor system. *SAE Tech. Pap.* **2009**. [CrossRef]
31. Martínez, T.L.M.; Sanz, O.; Centeno, M.A.; Odriozola, J.A. AISI 304 austenitic stainless steel monoliths: Modification of the oxidation layer and catalytic coatings after deposition and its catalytic implications. *Chem. Eng. J.* **2010**, *162*, 1082–1090. [CrossRef]
32. Bortolozzi, J.P.; Banús, E.D.; Milt, V.G.; Gutierrez, L.B.; Ulla, M.A. The significance of passivation treatments on AISI 314 foam pieces to be used as substrates for catalytic applications. *Appl. Surf. Sci.* **2010**, *257*, 495–502. [CrossRef]
33. Frías, D.M.; Nousir, S.; Barrio, I.; Montes, M.; Martínez, T.L.M.; Centeno, M.A.; Odriozola, J.A. Nucleation and growth of manganese oxides on metallic surfaces as a tool to prepare metallic monoliths. *Appl. Catal. A Gen.* **2007**, *325*, 205–212. [CrossRef]
34. Kołodziej, A.; Łojewska, J. Optimization of structured catalyst carriers for VOC combustion. *Catal. Today* **2005**, *105*, 378–384. [CrossRef]

35. Sun, H.; Zhang, Y.; Quan, X.; Chen, S.; Qu, Z.; Zhou, Y. Wire mesh honeycomb catalyst for selective catalytic reduction of NO_x under lean-burn conditions. *Catal. Today* **2008**, *139*, 130–134. [CrossRef]
36. Gómez, D.M.; Gatica, J.M.; Hernández Garrido, J.C.; Cifredo, G.A.; Montes, M.; Sanz, O.; Rebled, J.M.; Vidal, H. A novel CoO_x/La-modified-CeO_2 formulation for powdered and washcoated onto cordierite honeycomb catalysts with application in VOCs oxidation. *Appl. Catal. B Environ.* **2014**, *144*, 425–434. [CrossRef]
37. Payri, F.; Broatch, A.; Serrano, J.R.; Piqueras, P. Experimental-theoretical methodology for determination of inertial pressure drop distribution and pore structure properties in wall-flow diesel particulate filters (DPFs). *Energy* **2011**, *36*, 6731–6744. [CrossRef]
38. Jia, A.-P.; Jiang, S.-Y.; Lu, J.-Q.; Luo, M.-F. Study of catalytic activity at the CuO−CeO_2 interface for CO oxidation. *J. Phys. Chem. C* **2010**, *114*, 21605–21610. [CrossRef]
39. Mei, Z.; Li, Y.; Fan, M.; Zhao, L.; Zhao, J. Effect of the interactions between Pt species and ceria on Pt/ceria catalysts for water gas shift: The XPS studies. *Chem. Eng. J.* **2015**, *259*, 293–302. [CrossRef]
40. Jirátová, K.; Kovanda, F.; Balabánová, J.; Kšírová, P. Aluminum wire meshes coated with Co-Mn-Al and Co oxides as catalysts for deep ethanol oxidation. *Catal. Today* **2017**, 1–7. [CrossRef]
41. Amin, C.M.; Rathod, P.P.; Goswami, J.J. Copper based catalytic converter. *Int. J. Eng. Res. Technol.* **2012**, *1*, 1–6.
42. Kalam, M.A.; Masjuki, H.H.; Redzuan, M.; Mahlia, T.M.I.; Fuad, M.A.; Mohibah, M.; Halim, K.H.; Ishak, A.; Khair, M.; Shahrir, A.; et al. Development and test of a new catalytic converter for natural gas fuelled engine. *Sadhana—Acad. Proc. Eng. Sci.* **2009**, *34*, 467–481. [CrossRef]
43. Kumar, R.; Singh, S.; Kaur, M. Emission testing of catalytic converter using zirconium oxide (ZrO) and cobalt oxide (CoO) as catalyst. *Int. J. Mech. Prod. Eng. Res. Dev.* **2017**, *7*, 333–342.
44. Martínez T, L.M.; Sanz, O.; Domínguez, M.I.; Centeno, M.A.; Odriozola, J.A. AISI 304 Austenitic stainless steels monoliths for catalytic applications. *Chem. Eng. J.* **2009**, *148*, 191–200. [CrossRef]
45. Ihara, K.; Ohkubo, K.; Yasaki, S.; Yoshino, Y. Method of Manufacturing an Exhaust Gas Purifying Catalyst. U.S. Patent No. 5,208,206, 4 May 1993.
46. Flujometro Flujotech 250 y 600—HoracioResio.com. Available online: http://www.horacioresio.com/flujometro-flujotech-250-y-600/ (accessed on 7 December 2017).
47. Milt, V.G.; Banús, E.D.; Ulla, M.A.; Miró, E.E. Soot combustion and NO_x adsorption on Co,Ba,K/ZrO_2. *Catal. Today* **2008**, *133–135*, 435–440. [CrossRef]
48. Van Setten, B.A.A.L.; Schouten, J.M.; Makkee, M.; Moulijn, J.A. Realistic contact for soot with an oxidation catalyst for laboratory studies. *Appl. Catal. B Environ.* **2000**, *28*, 253–257. [CrossRef]